Long-Term Serviceability of Isotropically Reinforced Bridge Deck Slabs

GONGKANG FU, SREENIVAS ALAMPALLI, AND FRANK P. PEZZE III

Isotropically reinforced bridge decks have the potential to reduce costs to bridge owners for both construction and maintenance. For long-term serviceability evaluation, 13 such decks in New York State, with reinforcement ratios of 0.36 and 0.24 percent, have been inspected annually for the past 5 years; 4 of them have been load tested annually since they were constructed, the longest life being 8 years. Generally they have performed satisfactorily. Maximal stresses of bottom transverse rebars under 16-kip wheel loads over the years have always been below allowable levels based on conservative analyses. Rebar stresses in both the isotropic and AASHTO decks in New York State increase with age for the first year or two and remain relatively constant thereafter. Comparison of top-surface transverse cracking between the New York isotropic decks and North Carolina AASHTO decks indicates that the various reinforcement arrangements result in similar cracking severity.

In the United States, reinforced concrete (R/C) bridge deck slabs are designed on the basis of the flexural failure mode, according to the current AASHTO design code (*1*). However, extensive research has shown punching shear to be the dominant failure mode for slabs. This is attributed to flexural strength enhancement by the presence of membrane-compressive force in the slab, induced by its transverse boundary constraints, which is referred to as the "arching action" or the "dome effect." Based on varied research findings (*2–5*), Ontario had adopted an empirical design of isotropically reinforced deck slabs with a minimum reinforcement ratio of 0.3 percent in each face (*6*). This requires significantly less flexural steel than is required in the AASHTO code. Attracted by reductions in construction cost and probability of rebar corrosion resulting from this deck design of light reinforcement, researchers and state agencies in the United States have devoted notable efforts in this area over the past decade. A number of states have built or planned experimental isotropic deck slabs.

Slab capacity increase by arching action was noted as early as 1909 (*7*). Most early research in this area was oriented toward building-floor applications. Early work in this field has been briefly reviewed by several authors (*8–13*).

Behavior and strength of R/C bridge decks under static load are obviously of essential interest to bridge designers and owners. Modern studies of R/C bridge deck slabs in this area began at Queen's University in Ontario, Canada (*2,3,5,14*). They demonstrated excessive reserve strength of conventional R/C decks designed in accordance with the AASHTO provisions (*1*) by ⅛-scale models, and dominant punching failure of both isotropic and AASHTO orthotropic decks. After examining isotropic decks of various reinforcement ratios, they recommended an isotropic deck design with a minimum reinforcement ratio of 0.2 percent that possessed an adequate safety factor. Their findings were later confirmed by full-scale bridge testing (*15,16*), with 0.3 percent reinforcement adopted by the Ontario code (*6*). In the United States, Beal (*17,18*) confirmed these previous findings by testing ⅙-scale models and full-scale bridge decks containing isotropic and AASHTO orthotropic reinforcement. He also concluded that rebar stresses under the AASHTO design wheel load (20.8 kips) were lower than those predicted by the AASHTO code, and that ultimate strengths were six times larger than the design load in 0.25 percent reinforced isotropic deck models. Fang et al. (*8,9*) tested a full-scale isotropic deck model with about 0.4 percent reinforcement in each layer under simulated vehicle wheel loads. They found significant compressive membrane forces after cracking of the deck under load, with the deck behaving linearly up to a wheel load three times the AASHTO design load. Perdikaris and Beim (*10,11*) also confirmed adequate safety factors for isotropic decks by testing ⅙- and ⅓-scale deck models with 0.3 percent reinforcement, as well as their failure by punching shear. Puckett et al. (*19*) recently tested two full-scale decks—one reinforced according to the AASHTO code and the other 0.3 percent isotropically according to the Ontario code (*6*)—under vehicular loads at numerous locations. They found that bottom transverse rebars between girders experienced highest stresses under these loads. Jackson and Cope (*13*) tested two ½-scale models of isotropic deck to examine global load effects under wheel loads simulating critical vehicle loading cases. One deck had approximately 20 percent more reinforcement than is required by the Ontario code; the other was lighter. They found that the empirical design approaches of isotropic reinforcement appeared to be satisfactory, although global transverse moments could have large effects on deck behavior at various load levels.

Besides static strength, R/C deck fatigue strength has also been studied by several researchers. Batchelor et al. (*4,20*) performed fatigue tests on isotropic and orthotropic deck models of ⅛ scale under a sinusoidal concentrated load. They found that failure under fatigue load was always by punching shear. On the basis of their test results, they recommended an endurance limit of 0.4 (a fatigue load factor of 2.5) for an isotropic deck design with 0.2 percent reinforcement. Using fixed pulsating and stepwise moving loads, Okada et al. (*21*) and Sonoda and Horikawa (*22*) tested (a) full-scale models and panels sawed from distressed orthotropic decks and (b) 1.32 percent (top and bottom) isotropically reinforced slab models of ⅓ scale. First they found that moving load was substantially

Engineering Research and Development Bureau, New York State Department of Transportation, State Campus, Albany, N.Y. 12232.

more damaging than fixed pulsating load with respect to slab flexural and shear resistance. Fang et al. (*8,9*) tested a full-scale isotropic deck model with about 0.4 percent reinforcement under fixed pulsating 26-kip loads. They concluded that 5 million cycles of this pulsating load did not deteriorate the deck significantly. Perdikaris and Beim (*10,11*) first used constant rolling wheel load in their fatigue tests of ⅙-scale isotropic deck models with 0.3 percent reinforcement. The constant rolling wheel load resulted in a gridlike crack pattern on the model bottom surface, as often observed on decks in service (*10,11,21*). They also found that the constant rolling wheel load simulating real traffic loading is much more deteriorative than the fixed pulsating wheel load. It was concluded that the isotropic decks possess higher ductility and fatigue strength under constant rolling wheel load than the AASHTO orthotropic decks. Agarwal (*23*) reported a study of testing 14 Ontario isotropic and AASHTO bridge decks built for comparison in the early 1980s. He found that after a number of years of service, the slab panels displayed no visible signs of distress under wheel loads far exceeding factored loads specified by the codes (*1,6*). He further concluded that the major parameters affecting strength and stiffness are slab thickness, girder type, and girder spacing.

These results show that empirically designed isotropic decks with less steel possess adequate strengths higher than is conventionally predicted, but their long-term serviceability is subject to further examination. In general, service fatigue conditions of R/C bridge decks are much more severe than the laboratory environment in which most of these experimental studies were conducted. This is caused by thermal effects resulting from environmental temperature fluctuation, application of deicing chemicals, freeze-thaw cycling, damage cumulation caused by interaction of these deteriorating factors, and so forth. It is extremely difficult, if not impossible, to simulate these influencing factors in a laboratory. This paper presents a study partially sponsored by FHWA to examine long-term serviceability of full-scale isotropic deck slabs. It is intended to evaluate isotropic deck slabs based on their continuous in-service behavior.

SCOPE

Upon confirmation of previous research results regarding strength of isotropic decks, New York State experimented with an empirical isotropic deck design (*18*). Its cross section is shown with two rebar spacings—namely, 8 or 12 in. at centers with reinforcement ratios (of steel to effective cross section) of 0.36 and 0.24 percent, respectively (Figure 1). To take advantage of potential mass production of the reinforcing mat, the following provisions (*18*) applied:

1. A maximum girder spacing of 10 ft (i.e., a maximum ratio of girder spacing to deck thickness of 14.1) with no fewer than four girders.
2. Grade 60 steel with the top-mat epoxy coated,
3. Structural concrete Type E (water-cement ratio of 0.44; air content of 6.5 percent; slump, 3 to 4 in.; sand, 35.8 percent; and cement, 648 lb/yd^3) according to current New York State construction specifications (*24*),
4. Longitudinal bars parallel to girders and transverse bars parallel to the skew angle up to 30 degrees,

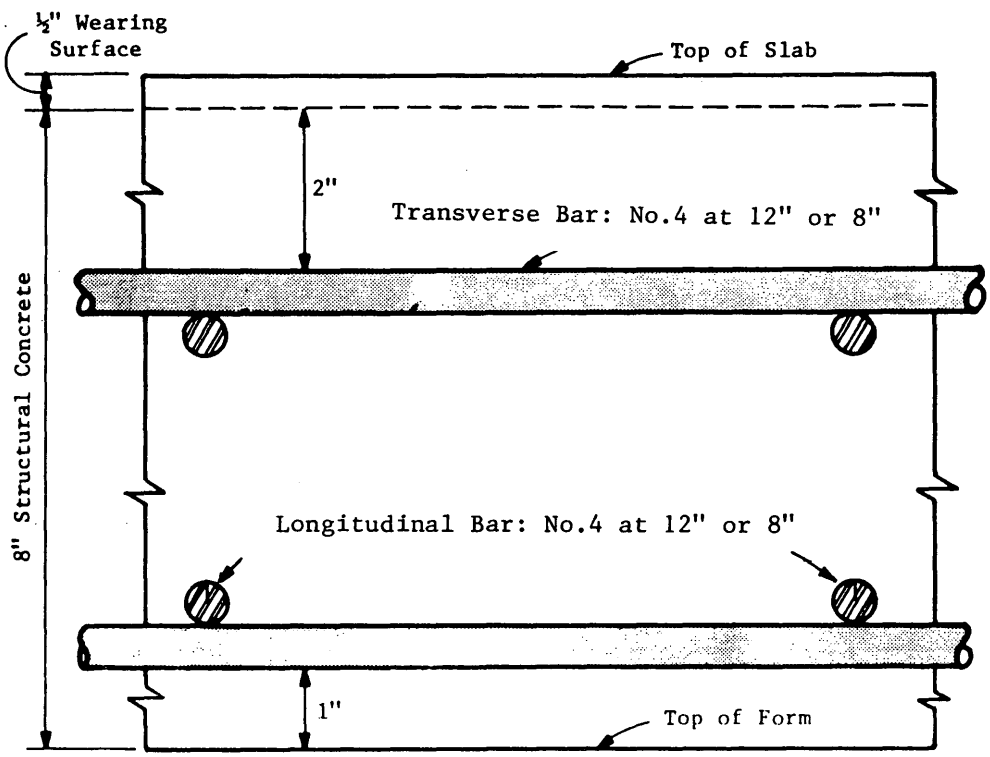

FIGURE 1 Standard cross section of isotropic decks in New York State.

5. Additional reinforcement for fascia overhang and negative moment areas according to the AASHTO specifications (*1*), and
6. Permissible metal stay-in-place forms according to New York State's current practice.

Since 1982, a total of 29 such isotropic decks have been constructed on bridges of multiple steel girders with diaphragms or cross bracings. Thirteen relatively older decks of the 29 are covered by the present study. Their locations are shown in Figure 2. Note that there are two bridges (sites) each at locations on Route 104 and the Hutchinson River Parkway. More details of the experimental isotropic decks are given in Table 1, including year built, average daily truck traffic, and structural features. As indicated in Table 1, 4 of the 13 bridges are instrumented with electrical resistance strain gauges.

Serviceability of concrete structural components refers to various aspects of their behavior under service conditions, such as deflection and stress level induced by service load, cracking behavior, and surface conditions affected by concrete cracking, spalling, and delamination. In this study, rebar stress levels under vehicular service load and surface conditions of the bridge decks were chosen for the serviceability evaluation. Stress level provides direct information on distress condition and available fatigue strength, and surface condition relates to corrosion probability with respect to accessibility of corrosive deicing chemicals to rebars. Deflection was not used as a criterion here because points of interest are not always accessible on a bridge in service without specially built equipment.

To obtain stress under wheel loads, the four instrumented experimental decks were load tested annually from construction until the present or until failure of aged strain gauges in the decks. Since 1986, when the oldest experimental deck (Site 1) had been in service for 4 years, the 13 experimental decks have been inspected annually to examine and record their surface condition with respect to serviceability.

LOAD TESTS AND REBAR STRESS UNDER SERVICE LOAD

Instrumentation and Load Test

Three types of load were applied to obtain deck rebar strain/stress under the AASHTO wheel load: (a) a single concentrated load distributed over an 8- × 20-in. plate by jacking a truck's rear axle (referred to as the simulated wheel load test); (b) a stationary vehicular wheel load at various longitudinal locations across the bridges (referred to as the static influence line test); and (c) a moving vehicular wheel load across the bridges at crawl speed (referred to as the dynamic influence line test). The wheel loads were applied along the centerline between two interior girders to produce maximum strain/stress in the instrumented rebars. Each loading was generally applied three times to produce replicates to eliminate possible instrumental error and accommodate unavoidable variations in vehicular loading. The simulated wheel load test was discontinued in 1987 because its results were regarded as having little value with respect to service load effects, considering the load's unrealistic distribution area and magnitude. Rebar strain readings in the static influence line test were recorded by a static data-acquisition system of 99 channels, whereas those in the dynamic influence line test used a dynamic data-acquisition system of eight channels at a speed

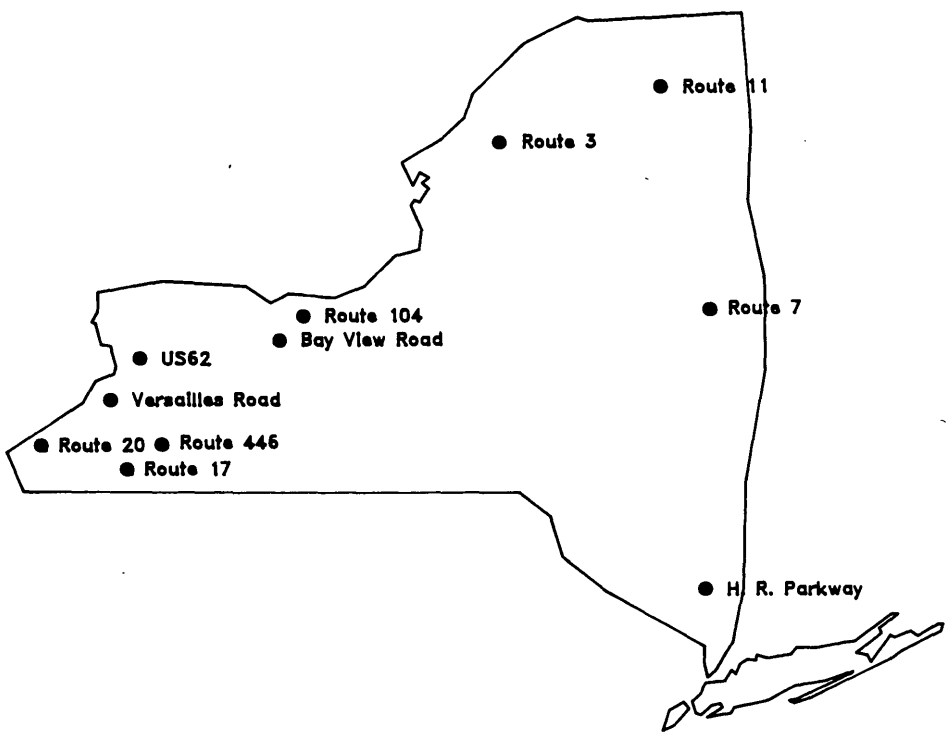

FIGURE 2 Locations of isotropic bridge decks in New York State.

TABLE 1 Background Data on New York State Isotropic Decks

Site	Location	Rebar Pattern[a]	Year Built	Truck Volume[b]	Skew, deg	Span Type	Span Length, ft	Girder Spacing
1a*	Bay View Rd	A	1982	NA	14	S	60,60,48,38	8'9"
1b*	Bay View Rd	12	1982	NA	14	S	60,38	8'9"
1c*	Bay View Rd	8	1982	NA	14	S	60,38	8'9"
2a*	Rte 7	A	1983	1300	50	S	131	10'0"
2b*	Rte 7	12	1983	1300	50	S	131	10'0"
2c*	Rte 7	8	1983	1300	50	S	131	10'0"
3*	Rte 20	12	1987	480	0	C	1030	9'10"
4	HR Parkway SB	12	1985	0	R	S	145	8'3"
5	HR Parkway NB	12	1986	0	R	S	144	8'0"
6	Rte 3	12	1986	280	12	S	176	10'0"
7	Rte 104 EB	12	1985	1050	8	S	150	9'0"
8	Rte 104 WB	12	1985	1050	8	S	150	9'0"
9	Rte 17	12	1986	1700	9	S	140	8'3"
10	US 62	12	1986	860	0	C	322	9'0"
11	Rte 446	12	1986	280	20	S	103	9'6"
12	Versailles Rd	12	1986	50	0	C	411	7'0"
13*	Rte 11	12	1988	470	0	C	756	9'0"

*Instrumented decks, R = skew varies because girder spacing varies from end to end, C = continuous, S = simple, NA = not available.

[a] A = AASHTO grid, 12 = 12x12 grid, 8 = 8x8 grid.

[b] Estimated annual daily truck traffic, from traffic volume reports of the Data Services Bureau, New York State Department of Transportation.

NOTES: Sites 1, 7, and 8 had removable forms. Sites 4, 5, 6, 9, 10, 11, and 12 have metal stay-in-place forms (SIPFs). Sites 3 and 13 have SIPFs with 0.2 and 0.1 percent, respectively, of the form area removed at gage locations. Site 2 has SIPFs, with 20 percent of the form area removed at the 12x12 grid gage location, 34 percent at the AASHTO grid gage location, and 17 percent at the 8x8 grid gage location.

of 25 samples per second. The dynamic influence line test was used to reduce test time, compared with the static influence line test. The two different influence line tests produced consistent results.

Figures 3 through 6 show instrumentation details for the four instrumented experimental decks, including types and locations of strain gauges. They were selected to monitor rebar strain/stress in critical areas. The instrumented bars are 4 to 6 ft long, including 15 in. at each end for overlapping with regular rebars. It is shown that Sites 1 and 2 have AASHTO orthotropic and the two isotropic (8- and 12-in. grid) reinforcement arrangements for behavior comparison. They are respectively referred to as Sites 1a, 1b, 1c, 2a, 2b, and 2c, as presented in Table 1.

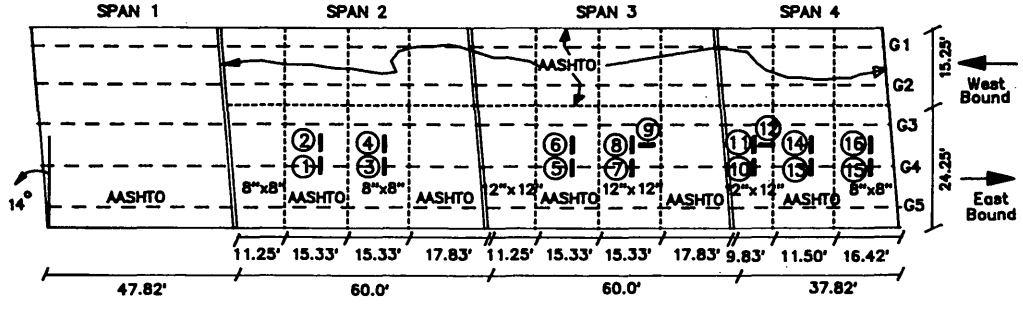

NOTES:

1. All spans are simply supported.
2. — = gage locations.
3. 16 four-arm strain gages of self-temperature compensating type for rebar uniaxial strain. Top transverse bars over girder G4: Nos. 1, 3, 5, 7, 10, 13, 15. Bottom transverse bars at center of interior bay: Nos. 2, 4, 6, 8, 11, 14, 16. Bottom longitudinal bars at center of interior bay: Nos. 9, 12.

FIGURE 3 Gauge locations at Site 1 (Bay View Road).

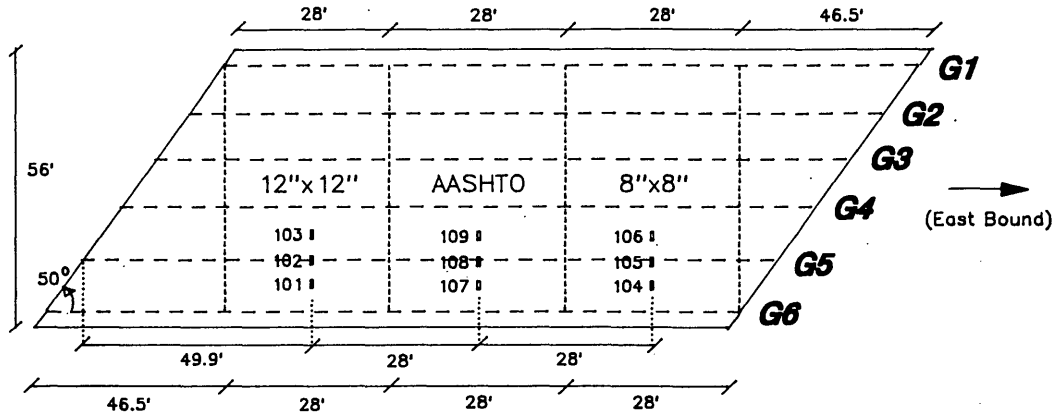

NOTES:

1. The span is simply supported.
2. ▮ = gage locations.
3. 9 four-arm strain gages of self-temperature compensating type for rebar uniaxial strain. Bottom transverse bars at center of fascia bay: Nos. 101, 104, 107. Top transverse bars over girder G5: Nos. 102, 105, 108. Bottom transverse bars at center of interior bay: Nos. 103, 106, 109.

FIGURE 4 Gauge locations at Site 2 (Route 7).

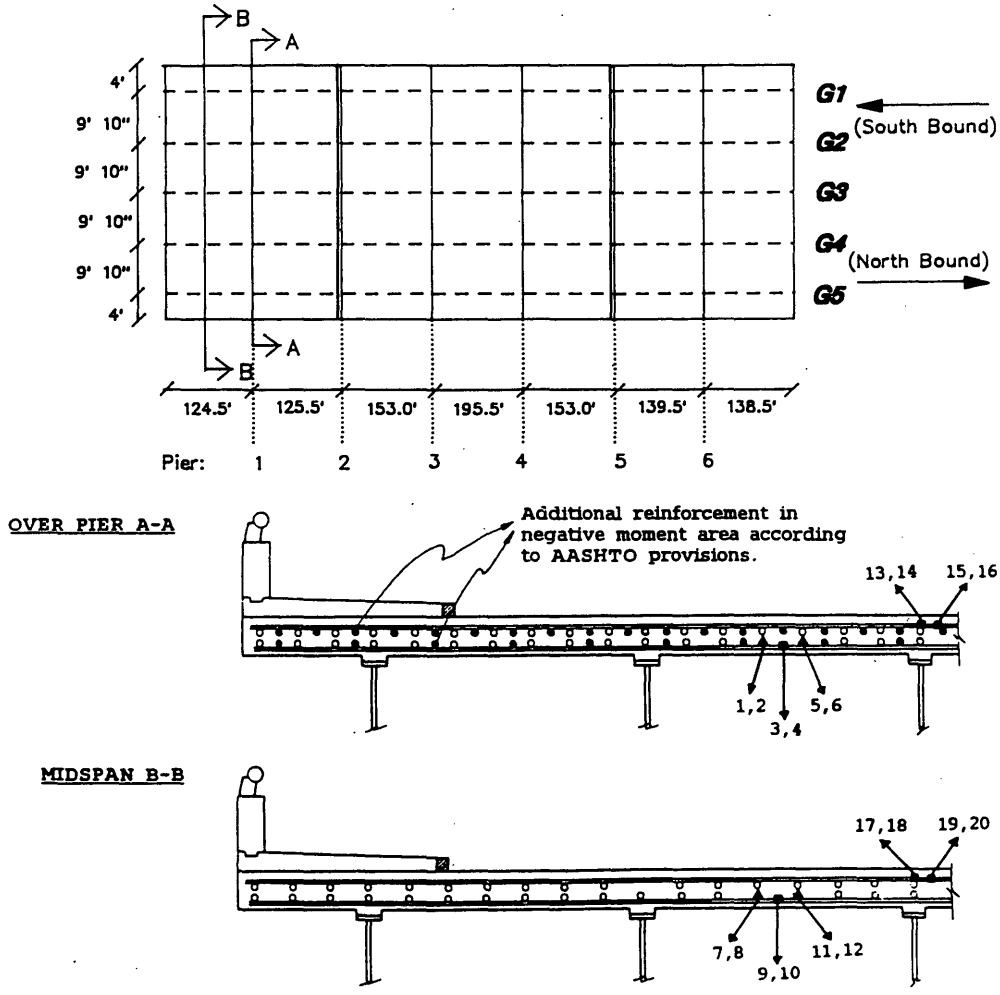

Notes:

■ Gage on Transverse Rebar
▲ Gage on Longitudinal Rebar
Total of 20 weldable single-arm strain gages of self-temperature compensating type. At each location, two gages on diametrically opposite sides of a rebar for uniaxial strain.

FIGURE 5 Gauge locations at Site 3 (Route 20).

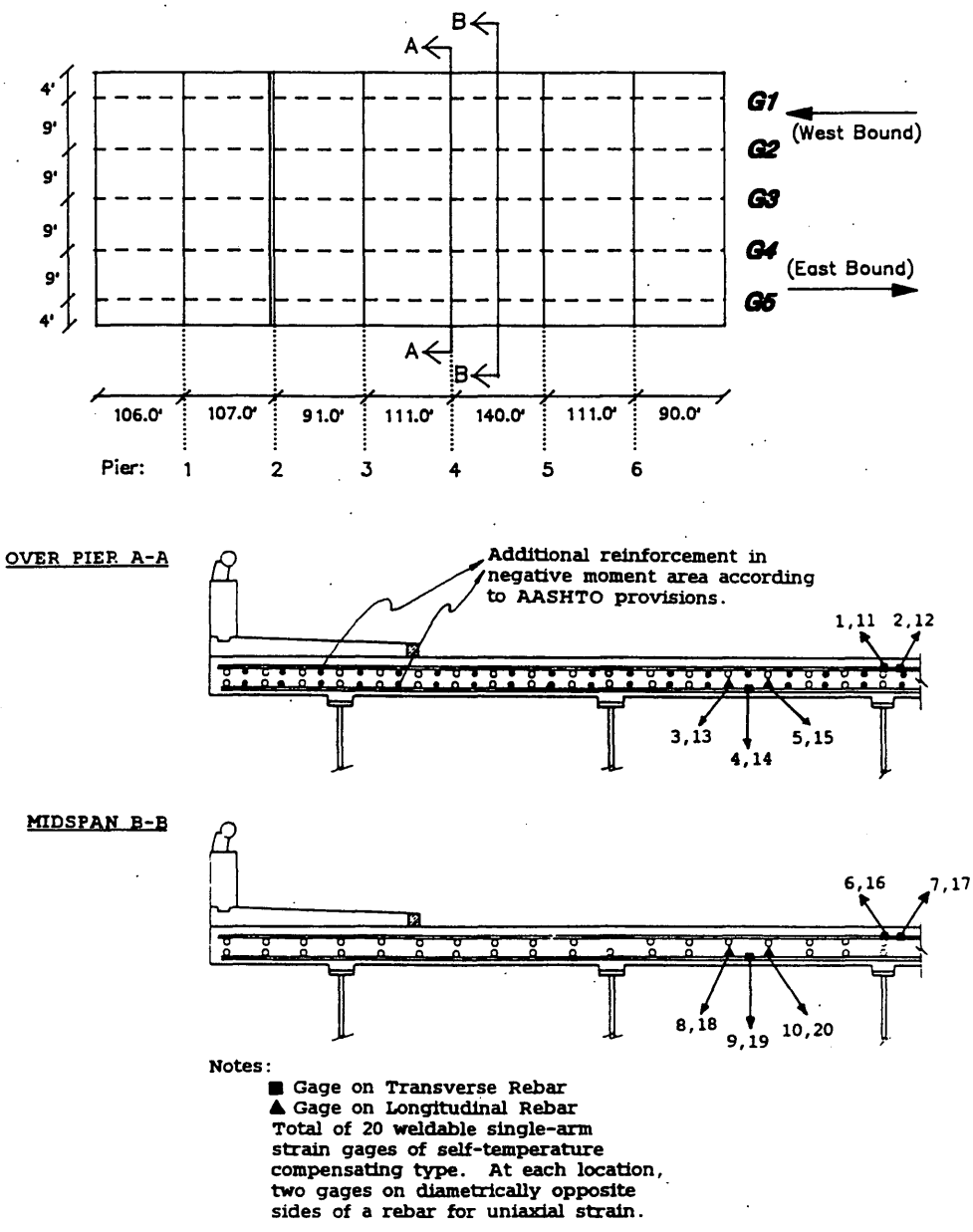

FIGURE 6 Gauge locations at Site 13 (Route 11).

Rebar Stress Under Service Load

Figure 7*a* and *b* shows typical rebar stress influence lines, obtained in a dynamic influence line load test at Site 3 (Route 20) in 1990. They show rebar stresses at sections of midspan and pier (Figure 5 shows more details of gauge locations). In the test a two-axle truck applied load, with front and rear axles of 15 and 30 kips, respectively, at a spacing of 15 ft. The truck was driven on the southbound side of the bridge, from Pier 2 to the south abutment, at a speed of about 10 mph. This section of the bridge is continuous over Pier 1 (Figure 5). The stresses obtained under the load were then linearly scaled to a vehicular load of 16-kip rear wheels. The abscissa in both figures is the distance from the front axle to the starting point near Pier 2. Figure 7*a* and *b* shows that the dynamic effects of the moving vehicle were minimized by the crawl speed. The figure also shows that rebar stresses consist of two components: global and local contributions. The local contribution is described by two sharp peaks induced by the front and rear wheels. The global one is demonstrated by curves of relatively lower slopes before and after the sharp peaks, which describe the deck's participation in load carrying as part of the bridge's cross section. In these two figures, the local effect in maximum rebar stresses is shown to be greater than the global effect.

In Figure 7*a*, stress of the bottom transverse bars (average of Gauges 9 and 10) at midspan section was contributed mainly by the global stress, except between distances of 170 and 210

ft. When the loading vehicle was on the adjacent span (between Piers 2 and 1), the bottom transverse bar at midspan was subjected to very low negative (compressive) stresses. This stress became positive (tensile) when the vehicle was on the gauged span (between Pier 1 and the south abutment). It is also shown in Figure 7*a* that the top transverse bars over an interior girder (Gauges 17 and 19) had much lower stresses than the bottom transverse one and yet experienced combined global and local effects. Rebar stresses at Gauges 7, 8, 11, 12, 18, and 20 are not shown here because of failure due to age, but previous results showed that their maximums were as negligibly low as about 0.64 ksi (*25*).

Figure 7*b* shows similar superposition of global and local effects of the vehicular wheel loads at the Pier 1 section indicated in Figure 5. It is seen that longitudinal bar stresses (Gauges 1, 5, and 6) were more localized than those of the transverse bars (Gauges 3 and 4), as indicated by the sharper peaks. Figure 7*b* also shows that the bottom longitudinal bars experienced higher stress than the bottom transverse bar. This stress was caused by the presence of a transverse crack on the top surface at the pier section. Without this crack, previous stress data showed that the opposite was true (*25*). Nevertheless, the highest stress shown in Figure 7*a* and *b* is lower than 3 ksi, apparently far below an allowable level.

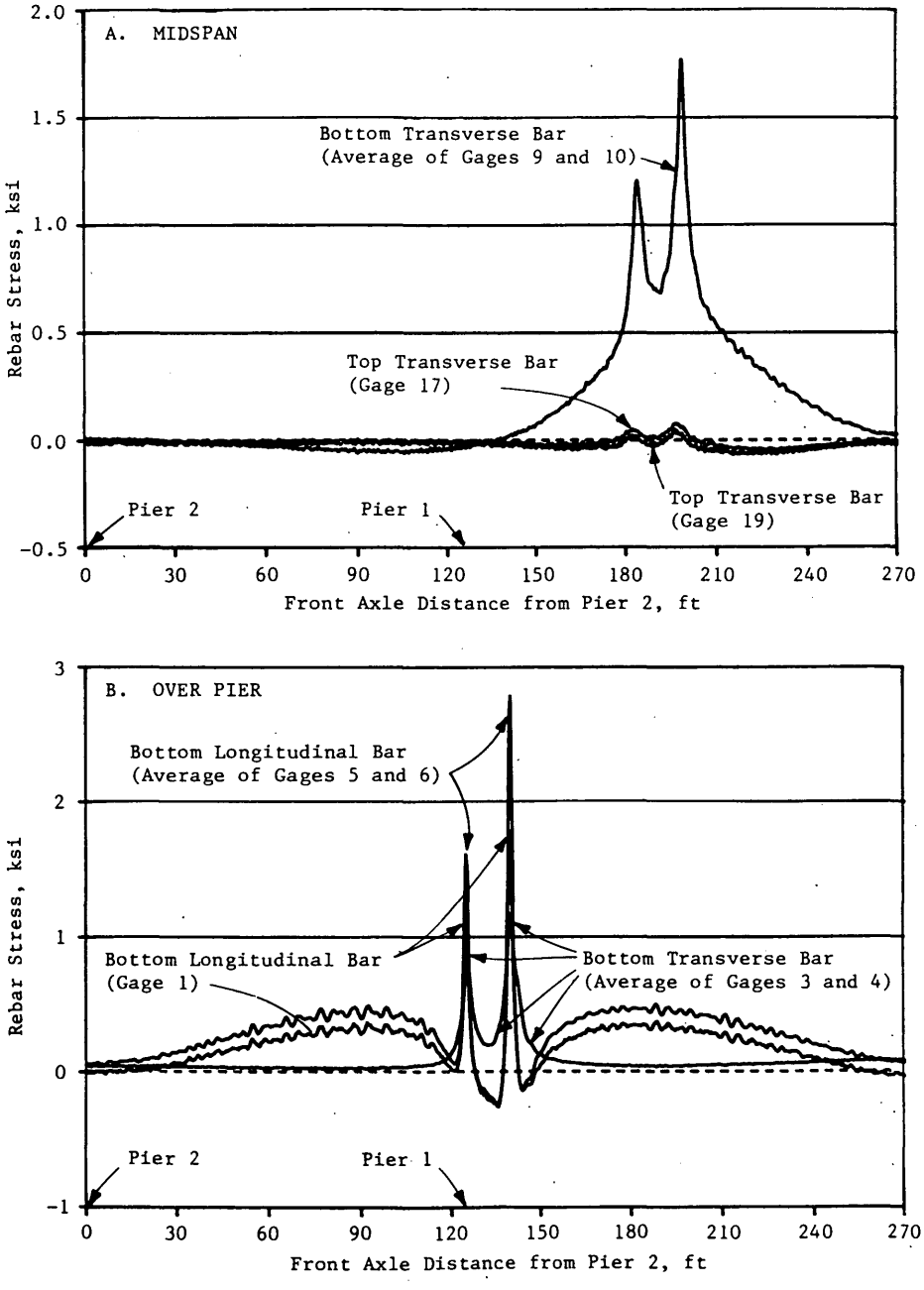

FIGURE 7 Site 3 influence lines under vehicular 16-kip rear wheel load.

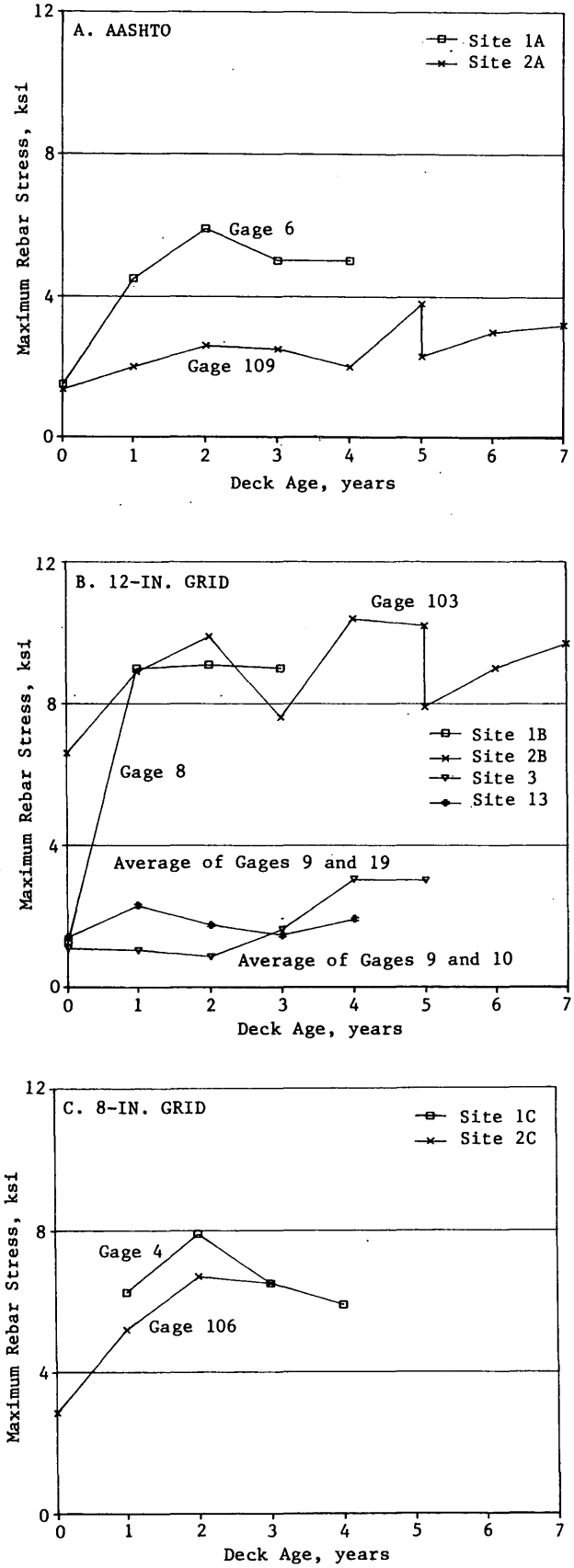

FIGURE 8 Maximum rebar stresses on bottom transverse bar under 16-kip wheel load.

TABLE 2 Comparison of Isotropic Deck Rebar Stresses

	12x12 Grid				8x8 Grid	
Live-Load Stress, ksi	Site 1b	Site 2b	Site 3	Site 13	Site 1c	Site 2c
Allowable[a]	14.3	12.9	14.6	14.6	15.7	14.8
Measured[b]	9.1	10.4	1.6	2.3	7.9	6.7

[a]Allowable live-load stress = (24 ksi - dead-load stress)/1.3.
[b]Measured live-load stress = maximum stress under vehicular 16-kip wheel load obtained in the load tests.

Stress at Gauges 2, 13, 14, 15, and 16 was not obtained in the 1990 test because of their failure. It is noted that by 1990 this deck had been in service for 4 years. Previous rebar stresses were lower than those presented in Figure 7*a* and *b*.

Figure 8*a*, *b*, and *c* demonstrates evolution of maximal stresses in bottom transverse bars with deck age, for the three reinforcement arrangements. Comparison of these curves shows that the 12-in. grid experienced higher stress than the other two patterns of reinforcement at Sites 1 and 2. This is expected since less steel was used in the 12-in. grid. It is noted that, at a deck age of 5 years, two tests were performed in Site 2 (Route 7), and two stress readings were recorded in Figure 8*a* and *b*. These different readings characterize variation of the stress results over deck age as shown in these figures. This variation is attributed to several factors: uncertainty in paths of the loading vehicle, possible nonlinearity in deck load-response relationship under various levels of applied loads, and/or possible electrical noise influencing data recording. This variation is unavoidable in a field-testing environment and is not a cause for concern. Despite the variation, a clear tendency is observed in Figure 8*a* through *c* that rebar stresses increased in the first year or two of service and remained relatively constant thereafter, regardless of reinforcement arrangements.

The global maximum stresses of 12-in. and 8-in. grid decks shown in Figure 8*b* and *c* are listed in Table 2. Using a simplified model of transversely continuous beam and the AASHTO allowable stress method (*1*), dead-load stresses in the transverse rebar were found for the instrumented decks, under a uniformly distributed dead load of 142 lb/ft^2 (accounting for weights of the deck, stay-in-place forms, and future overlay). Allowable live-load rebar stresses are computed as the differences between a total allowable stress of 24 ksi for Grade 60 steel and the dead-load stresses, with the maximum impact factor 1.3 by the AASHTO code considered conservatively. These are also listed in Table 2 for comparison. On the basis of the conservative analyses, measured maximal stresses are all lower than allowable levels for the two isotropic reinforcement arrangements.

GENERAL INSPECTION

Since 1986, the 13 experimental isotropic decks have been inspected for possible deterioration affecting serviceability.

They are examined for cracking, spalling, and delamination by visual and sonic (chain-drag) methods. Both top and bottom deck surfaces are inspected. No spalling or delamination have been observed. Generally, cracking is judged to be minor and the decks have performed satisfactorily (*26*).

At Sites 1 and 2, a few bottom transverse cracks highlighted by efflorescence are seen from the ground. These cracks appear in similar intensities in all sections regardless of reinforcement (AASHTO, 12-in. or 8-in. grids). Sites 7 and 8 have more intensive bottom transverse and longitudinal cracks, which are highly visible. These two sites will be discussed further, along with top surface inspection data. These four are the only bridges among the 13 addressed here with forms either completely or partially removed so that their bottom surface could be inspected. Top surface cracking at all the sites will also be discussed in more detail.

Cracking on upper deck surface is classified in three types according to direction of extension: transverse, longitudinal, or diagonal. Transverse cracks are defined as perpendicular to traffic flow and longitudinal as parallel to traffic flow. All others are noted as diagonal. Examination and recording of cold-joint cracking at the ends of concrete pours were discontinued in 1989, because this was considered unavoidable and irrelevant to reinforcement arrangement. Crack density, defined as crack length per unit area (inches per square yard), is used for quantitative measurement of cracking severity.

Transverse cracking was predominant and longitudinal much less frequent (64 and 32 percent, respectively, in 1990). Figure 9 relates total crack densities for individual decks to age. Top surface cracking generally increases with age in both isotropic and AASHTO decks. Note, however, that crack densities actually decreased with age once for Sites 2a, 6, and 13, apparently because of either inexperience of the inspectors or reduction of crack visibility by less moisture near the deck surface at inspection time. Since most observed cracks are hairline or narrower, these two factors did affect inspection results for crack density. Although Sites 1, 7, and 8 have relatively higher crack densities, the decks are generally performing satisfactorily.

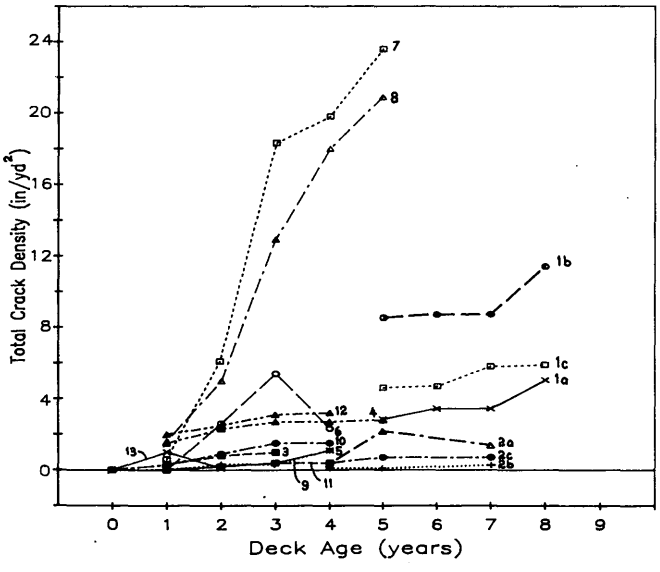

FIGURE 9 Total crack densities on top surface of experimental decks.

Site 1 experienced the third highest crack density (Figure 9). Note that this bridge was subjected to the simulated wheel loads in early tests of as high as 30 kips over an 8- × 20-in. area. Most cracks observed here are near loading plate areas.

Figure 9 also shows that Sites 7 and 8 experienced the highest crack densities; 65 and 62 percent are transverse, and 31 and 36 percent longitudinal, respectively. These two bridges were constructed simultaneously by the same contractor in 1985. A special investigation attempted to identify causes of this relatively severe cracking. Two cores were taken in 1990 from Site 7 (Route 104 eastbound). Core 1 was at an intersection of longitudinal and diagonal cracks (also of longitudinal and transverse bars), and Core 2 over a longitudinal crack (also over a longitudinal bar) along the centerline between two interior girders. Epoxy coating of top bars in both cores was found to be intact; no corrosion was observed. In Core 1, the crack extended from the top surface about one-quarter into the deck's depth. Multiple aggregate fractures were found in Core 2, with a crack penetrating its full depth; this indicates that the longitudinal cracking was load related and occurred after the concrete developed its strength. Early concrete strengths at both sites were also found to have been sought by the contractor for early opening of the bridges. Generally this is done for the contractor's convenience for moving heavy construction equipment. Such movements may have caused the observed longitudinal cracks. Construction records also show that at each site two of eight tested slumps exceeded the maximum specified allowable level (*24*). Higher slump may cause more transverse cracking due to more severe concrete shrinkage. It was concluded that higher crack densities at Sites 7 and 8 were caused mainly by improper construction procedures and possible overloading.

In an investigation of North Carolina's AASHTO R/C decks (*27*), 72 bridges were inspected solely to determine the severity of transverse cracking. Of these, 15 were multiple-steel-girder bridges in a service age range comparable with that of New York's experimental decks, with results used here for comparison. Crack severity in that study was defined as a weighted number of cracks per unit of longitudinal length [cracks per linear foot (CLF)] equal to the total number of major transverse cracks plus 0.25 total number of minor transverse cracks per span length. Major cracks were defined as those propagating from at least one edge of the pavement to the roadway centerline, and minor, as shorter cracks. New York's crack density data were then converted to CLF values. In Table 3, New York's 12-in. grid isotropic decks and North Carolina's AASHTO decks are compared. This comparison shows that the highest AASHTO deck CLF is 0.266 versus 0.247 for the isotropic decks. Excluding the abnormal cases (Sites 7 and 8 in New York and 64-32-045E in North Carolina), average CLFs for the isotropic and AASHTO decks are 0.030 and 0.031, respectively. Their standard deviations are also equivalent (Table 3). Table 3 shows that transverse cracking severities of the isotropic and the AASHTO decks are generally equivalent.

TABLE 3 Comparison of Transverse Cracking

New York 12x12 Isotropic Decks				North Carolina AASHTO Decks		
Site	Location	Age, years	CLF*	Bridge	Age, years	CLF*
1	Bay View Rd	8	0.114	1835-44-088	3	0.000
2	Rte 7	7	0.007	231-32-020	9	0.000
3	Rte 20	3	0.014	53-44-015	3	0.000
4	HR Parkway SB	5	0.062	264-40-010	9	0.000
5	HR Parkway NB	4	0.026	64B-32-010	5	0.000
6	Rte 3	4	0.004	95-44-083N	3	0.026
7	Rte 104 EB	5	0.247	64B-32-010	5	0.013
8	Rte 104 WB	5	0.200	264-40-010	9	0.055
9	Rte 17	4	0.018	1655-40-060	3	0.008
10	US 62	4	0.021	8-60-030	1	0.053
11	Rte 446	4	0.000	95-44-083N	3	0.075
12	Versailles Rd	4	0.063	64-32-045E	4	0.266
13	Rte 11	2	0.001	85-60-100N	4	0.104
				85-60-090N	5	0.055
				220-55-012N	4	0.041
Mean**			0.030	Mean***		0.031
Standard Deviation**			0.036	Standard Deviation***		0.034

*CLF = cracks per linear foot = (total major transverse cracks + total minor transverse cracks/4)/span length.
**Excluding Sites 7 and 8.
***Excluding Site 64-32-045E.

CONCLUSIONS

The strength of empirically designed isotropic decks has been verified in previous research as adequate for current wheel loading. Their long-term serviceability, when subjected to severe service fatigue conditions remains an issue to be addressed. Thirteen experimental isotropic decks in New York State have been examined periodically by both load test and general inspection over their service lives, with the longest open for 8 years. No spalling or delamination has been found and cracking is judged to be minor. Isotropic decks experienced crack severity comparable with that of AASHTO decks. Maximum rebar stresses in the isotropic decks under the AASHTO wheel load of 16 kips are always lower than allowable levels on the basis of conservative analyses. Transverse cracking severity of the isotropic and AASHTO decks is found to be equivalent. Maximal transverse rebar stresses under the 16-kip wheel load increased for the first year or two of service and remained relatively constant thereafter, regardless of reinforcement patterns.

ACKNOWLEDGMENTS

The study presented here was partially supported by FHWA. The assistance and cooperation of New York State Department of Transportation personnel over the years are gratefully appreciated. Discussions with D. B. Beal and M. J. Loftus were particularly useful.

REFERENCES

1. *Standard Specifications for Highway Bridges*, 13th ed. AASHTO, Washington, D.C., 1983.
2. B. E. Hewitt. *An Investigation of the Punching Strength of Restrained Slabs with Particular Reference to the Deck Slabs of Composite I-Beam Bridges*. Ph.D. dissertation. Queen's University at Kingston, Ontario, Canada, March 1972.
3. B. E. Hewitt and B. deV. Batchelor. Punching Shear Strength of Restrained Slabs. *Journal of the Structural Division*, ASCE, Vol. 101, No. 9, 1975, pp. 1837–1853.
4. B. deV. Batchelor, B. E. Hewitt, and P. Csagoly. An Investigation of the Fatigue Strength of Deck Slabs of Composite Steel/Concrete Bridges. In *Transportation Research Record 664*, TRB, National Research Council, Washington, D.C., 1978, pp. 153–161.
5. B. deV. Batchelor, B. E. Hewitt, P. Csagoly, and M. Holowka. Investigation of the Ultimate Strength of Deck Slabs of Composite Steel/Concrete Bridges. In *Transportation Research Record 664*, TRB, National Research Council, Washington, D.C., 1978, pp. 162–170.
6. *Ontario Highway Bridge Design Code*, 2nd ed. Ministry of Transportation and Communications, Downsview, Ontario, Canada, 1983.
7. C. A. Turner. Advance in Reinforced-Concrete Construction: An Argument for Multiple-Way Reinforcement in Floor-Slabs. *Engineering News*, Vol. 6, No. 7, 1909, pp. 178–181.
8. I.-K. Fang. *Behavior of Ontario-Type Bridge Deck on Steel Girders*. Ph.D. thesis. University of Texas at Austin, 1985.
9. I.-K. Fang, J. Worley, N. H. Burns, and R. E. Klingner. Behavior of Isotropic R/C Bridge Decks on Steel Girders. *Journal of Structural Engineering*, ASCE, Vol. 116, No. 3, 1990, pp. 659–678.
10. P. C. Perdikaris and S. Beim. RC Bridge Decks under Pulsating and Moving Load. *Journal of Structural Engineering*, ASCE, Vol. 114, No. 3, 1988, pp. 591–607.
11. P. C. Perdikaris and S. Beim. *Design of Concrete Bridge Decks*. Report FHWA/OH-88/004. Department of Civil Engineering, Case Western Reserve University, Cleveland, Ohio, 1988.
12. J. A. Puckett, J. D. Lohrer, and R. D. Naiknavare. *Evaluation of Bridge Deck Utilizing Ontario Bridge Deck Design Method: Instrumentation and Testing of Two Reinforced Concrete Bridge Decks*, Vol. 2. Report FHWA/WY-89-002. Department of Civil Engineering, University of Wyoming, Laramie, and Wyoming Highway Department, July 1989.

13. P. A. Jackson and R. J. Cope. The Behavior of Bridge Deck Slabs under Full Global Load. In *Developments in Short and Medium Span Bridge Engineering '90* (B. Bakht, R. A. Dorton, and L. G. Jaeger, eds.), Toronto, Ontario, Canada, 1990, Vol. 1, pp. 253–265.
14. P. Y. Tong and B. deV. Batchelor. Compressive Membrane Enhancement in Two-way Bridge Slabs. In *Cracking, Deflection, and Ultimate Load of Concrete Slab System* (E. G. Nawy, ed.), ACI Special Publication SP-30, Paper SP30-12. American Concrete Institute, 1971, pp. 271–286.
15. M. Holowka. *Testing of a Trapezoidal Box Girder Bridge*. Report RR221. Ministry of Transportation and Communications, Downsview, Ontario, Canada, Nov. 1979.
16. M. Holowka and P. Csagoly. *Testing of a Composite Prestressed Concrete AASHTO Girder Bridge*. Report RR222. Ontario Ministry of Transportation and Communication, July 1980.
17. D. B. Beal. Load Capacity of Concrete Bridge Decks. *ASCE Journal of Structural Division*, ASCE, Vol. 108, No. 4, 1982, pp. 814–832.
18. D. B. Beal. *Reinforcement for Concrete Bridge Decks*. Research Report 105. Engineering Research and Development Bureau, New York State Department of Transportation, July 1983.
19. J. A. Puckett, R. D. Naiknavare, and J. D. Lohrer. *Evaluation of Bridge Deck Utilizing Ontario Bridge Deck Design Method: Review of Experimental and Analytical Research in Lightly Reinforced Bridge Decks*, Vol. 1. Report FHWA-WY-89-002. Department of Civil Engineering, University of Wyoming, Laramie, and Wyoming Highway Department, July 1989.
20. B. deV. Batchelor and B. E. Hewitt. Are Composite Bridge Slabs Too Conservatively Designed?—Fatigue Studies. In *Fatigue of Concrete*. ACI Special Publication SP41, Paper SP41-15. American Concrete Institute, 1974, pp. 331–346.
21. K. Okada, H. Okamura, and K. Sonoda. Fatigue Failure Mechanism of Reinforced Concrete Bridge Deck Slabs. In *Transportation Research Record 664*, TRB, National Research Council, Washington, D.C., 1978, pp. 136–144.
22. K. Sonoda and T. Horikawa. Fatigue Strength of Reinforced Concrete Slabs Under Moving Loads. *Proc., IABSE Colloquium, Fatigue of Steel and Concrete Structures*, Lausanne, Switzerland, Vol. 37, 1982, pp. 455–462.
23. A. C. Agarwal. Load Testing of New Concrete Bridge Deck Slabs. In *Developments in Short and Medium Span Bridge Engineering '90* (B. Bakht, R. A. Dorton, and L. G. Jaeger, eds.), Toronto, Ontario, Canada, 1990, Vol. 1, pp. 277–289.
24. *Standard Specifications: Construction and Materials*. New York State Department of Transportation, Albany, Jan. 1985.
25. S. Alampalli and G. Fu. *Influence Line Tests of Isotropically Reinforced Bridge Deck Slabs*. Client Report 54. Engineering Research and Development Bureau, New York State Department of Transportation, Sept. 1991.
26. F. P. Pezze and G. Fu. *1990 Visual Inspection of Isotropic Bridge Decks*. Client Report 51. Engineering Research and Development Bureau, New York State Department of Transportation, May 1991.
27. G. R. Perfetti, D. W. Johnston, and W. L. Bingham. *Incidence Assessment of Transverse Cracking in Concrete Bridge Decks: Structural Considerations*. Vol. II. Report FHWA/NC/85-002. Center for Transportation Engineering Studies, North Carolina State University at Raleigh, June 1985.

Publication of this paper sponsored by Committee on General Structures.